IEEE Access
Multidisciplinary | Rapid Review | Open Access Journal

Received 28 August 2023, accepted 14 September 2023, date of publication 18 September 2023,
date of current version 18 October 2023.

Digital Object Identifier 10.1109/ACCESS.2023.3316880

RESEARCH ARTICLE

Optimal Scheduling of Integrated Electricity and Gas System Considering Gas-Fired Unit's Peak-Regulation Loss

CHANG LIU[1], YUNCHU WANG[1], YUANQIAN MA[1,2], YUN YANG[3], CHANGMING CHEN[1], ZHU CHAO[3], LI YANG[1], AND ZHENZHI LIN[1], (Senior Member, IEEE)

[1]School of Electrical Engineering, Zhejiang University, Hangzhou 310027, China
[2]School of Information Science and Engineering, Zhejiang Sci-Tech University, Hangzhou 310018, China
[3]Power Dispatching Control Center, Guangdong Power Grid Company Ltd., Guangzhou 510600, China

Corresponding author: Zhenzhi Lin (linzhenzhi@zju.edu.cn)

This work was supported in part by the Natural Science Foundation of China under Grant 52077195, in part by the Joint Funds of the National Science Foundation of China under Grant U2166206, and in part by the Science and Technology Program of China Southern Power Grid under Grant GDKJXM20200744.

ABSTRACT Under the background of dual-carbon goal, renewable energy-oriented power system and integrated energy are the trends of energy system. In order to cope with the uncertainty and volatility of renewable energy output, gas-fired unit can serve as a superior peak-regulation source to effectively solve the supply-demand mismatch problem. Nevertheless, rotor loss of gas-fired unit in the peak-regulation process weakens the operation performance and increases the practical cost of providing peak-regulation service. There is security risk of gas-fired unit in the peak-regulation process, especially during deep peak-regulation and startup/shutdown process, which leads to deficiency in the willingness to provide peak-regulation service. In this context, an optimal scheduling model of integrated electricity and gas system (IEGS) considering peak-regulation loss and renewable energy consumption is proposed in the paper. Firstly, peak-regulation loss and peak-regulation cost model is built under startup/shutdown regulation and variable-load regulation mode of gas-fired unit, respectively. On this basis, the optimal IEGS scheduling model taking gas-fired unit's peak-regulation loss and renewable energy consumption into account is established, aiming at minimizing the total scheduling cost including operation cost considering peak-regulation loss, renewable energy abandoning penalty, load shedding cost and carbon emission cost under gas network constraints, peak-regulation constraints and other constraints. Finally, a case study on a modified IEGS with a high proportion of renewable energy from Guangdong province, China is conducted to verify the effectiveness of the proposed model, and the simulation results demonstrate that the proposed model could obtain the higher renewable energy consumption level and less carbon emission, and could relieve the rotor loss of gas-fired unit.

INDEX TERMS Integrated electricity and gas system, peak-regulation loss, line-pack, renewable energy consumption.

NOMENCLATURE

$P_{\max}$	the maximum technical output of gas-fired unit.
$P_{s\min}$	the minimum technical output of startup/shutdown peak regulation.
$P_{d\min}$	the minimum technical output of basic regulation.
$P_{\lim}$	the limit output of deep regulation.
C_{ud}	gas consumption cost of gas-fired unit's starting-up or shutting-down.
V	the amount of gas consumed in each startup/shutdown process.
c_{gas}	the price of gas.
k	the yield limit ratio of the rotor.
K_{th}	thermal stress concentration coefficient of the rotor.

The associate editor coordinating the review of this manuscript and approving it for publication was Ali Raza.

σ_{eq}	the nominal equivalent stress of the rotor's shaft at the stress concentration part.
σ_0	high temperature yield limit of the rotor's shaft.
σ_{max}	the maximum stress of elastic groove bottom.
K_s	the plastic strain concentration coefficient of the rotor.
$\Delta\varepsilon_t$	the full strain of rotor in the startup/ shutdown process.
E	the elastic modulus of the rotor material.
N_s^{st}	the cracking cycle of rotor in startup/ shutdown process.
d_s^{st}	loss rate of a single startup or shutdown process.
S_g	price of gas-fired unit.
P_s/ P_d	output of gas-fired unit in startup-shutdown regulation/deep variable load regulation.
$T_{s,on}^t/T_{s,off}^t$	the startup/shutdown binary variable of gas-fired unit.
ΔT_m	the average temperature of rotor.
a	temperature conductivity coefficient.
η	temperature rise rate.
R	the radius of rotor.
α	expansion coefficient of rotor.
λ	the Poisson's ratio.
N_v	cracking cycle of deep variable load regulation.
φ	shrinkage coefficient of material's section.
σ_ω	limit of fatigue strength of material.
d_v	loss rate of deep variable load regulation.
V_{pur}^t	total amount of purchased natural gas excluding that consumed by gas-fired unit.
C_{maint}	maintenance cost of gas-fired unit.
c_{PV}/c_{WT}	penalty cost of per unit photovoltaic/ wind turbine power abandoned.
$P_{PV,wst}^t/P_{WT,wst}^t$	abandoned quantity of photovoltaic/ wind turbine power.
P_{cut}^t	amount of shed load.
c_{cut}	price of per unit load shedding.
$c_{carb}^{GS}/c_{carb}^{CHP}/$ $c_{carb}^{EH}/c_{carb}^{P2G}$	carbon emission cost for GS/CHP/EH/P2G.
S_d^{max}	the upper limit of deep variable load regulating capacity of unit d within a day.
N_s^{max}	the upper limit of startup and shutdown times within a day.
$T_{on}^{min}/T_{off}^{min}$	the minimum continuous operating time / shutdown time.
S_r^t	natural gas flow of source.
S_r^{max}/S_r^{min}	the upper and lower limit of gas source r's gas flow.
W_{GSS}^t	stored natural gas amount.
W_{GSS}^{max}	the upper limit of storing amount.
$W_{GSS,in}^t$ $/W_{GSS,out}^t$	stored and released gas.
$\eta_{GSS}^{in}/\eta_{GSS}^{out}$	storing and releasing efficiency.
$S_{l,in}^t/S_{l,out}^t$	inflow and outflow.
M_l^t	line pack of pipeline.
S_q^t	gas flow of compressor.
$S_q^{max}/.\ S_q^{min}$	the upper and lower limits of the gas flow allowed to flow through the compressor.
ζ_q^t	gas flow consumed by compressor.
K_q	gas consumption coefficient.
k_q^{max}/k_q^{min}	the upper / lower limits of compression ratio.
$\prod_{q,out}^t / \prod_{q,in}^t$	squared outflow/ inflow gas pressure of compressor.
Π_j^t	squared node pressure.
Π_j^{max}/Π_j^{min}	the upper and lower limits of squared node pressure.
$P_{CHP}^t/H_{CHP}^t/$ G_{CHP}^t	electric output/ thermal output / natural gas power of CHP.
$\eta_{CHP}^{G\text{-}H}/\eta_{CHP}^{H\text{-}E}$	natural gas-heat conversion efficiency / heat-electric conversion efficiency of CHP.
U_{CHP}^{max}	the upper limit of the climbing rate of CHP.
P_{GS}^t/G_{GS}^t	electric output power and natural gas input power of gas-fired unit.
U_s^t	binary variable of unit s at time t indicating operation state.
U_{GS}^{max}	the upper limit of the ramping rate of the unit.
H_{EB}^t/P_{EB}^t	heating power / electric power of EB.
$H_{EB}^{max}/H_{EB}^{min}$	the upper and lower limits of heating output power.
U_{EB}^{max}	the upper limit of EB's climbing rate.
P_{P2G}^t/G_{P2G}^t	electric power / natural gas output of P2G.
$P_{P2G}^{max}/P_{P2G}^{min}$	the upper and lower limits of P2G's electric power.
S^t	SOC value of ESDs.
$\gamma^{los}/\gamma^{cha}/\gamma^{dis}$	energy loss coefficient/ charging efficiency/ discharging efficiency of ESDs.
$\Delta t/T$	scheduling time interval/ the number of scheduling intervals.
M_{ES}	total capacity of the constructed ESDs.
P_{cha}^t/P_{dis}^t	charging power / discharging power of ESDs.
$\gamma_{max}/\gamma_{min}$	proportions of upper/ lower SOC in ESDs' total capacity.
$P_{cha}^{max}/P_{dis}^{max}$	the upper limits of charging / discharging power.
B_{cha}^t/B_{dis}^t	auxiliary binary variables of charging/ discharging.

I. INTRODUCTION

Under the dual-carbon background in China, establishing renewable energy oriented power system and realizing the collaborative utilization of various energy types have become the core mission of Chinese energy transformation [1], [2], [3]. At present, power system has entered the stage with a high proportion of renewable energy and the annual newly-installed capacity is dominated by renewable energy [4], [5], [6]. Characterized by fluctuation and randomness, the grid-connection of renewable energy leads to the mismatch of source and supply, which brings great challenges to the secure and stable operation of power system [7], [8], [9]. A large scale peak regulating power source is accordingly needed to smooth the fluctuations. Much work has been done on the participation of various power resources in peak-regulation: For example, in [10], a day-ahead optimal dispatch model of coupled system is established considering peak regulation ancillary services and ladder-type ramping rate constraint of thermal power unit based on its deep peak regulation characteristics. In [11], a controllable local peak-regulation strategy of effective utilization of the available plug-in electric vehicle battery capacity for peak-shaving. In [12], it is summarized that contributing a cooperation mechanism among multiple energy systems is an effective way to promote the peak regulation flexibility of gas-fired power plants. A coordinated peak regulation control strategy for energy storage and thermal power units is proposed in [13]. Among various peak-regulation units, gas-fired unit is a kind of peak-regulating power source with excellent comprehensive performance, which has the advantages of flexible operation, fast starting-up and shutting-down speed, fast ramping speed, outstanding peak-regulating performance and so on [14]. Therefore, developing gas-fired unit peak-regulation along with the development of renewable energy is the inevitable trend of renewable energy-oriented power system.

Gas-fired unit has the problems of limited heat channel components service life and high maintenance cost [15]. Working under the conditions of high temperature, high thermal stress, and high concentrated stress for a long time, the rotor of gas-fired unit tends to wear and determines the service life of the unit [16]. When gas-fired unit is in the process of changing output dramatically and starting-up/ shutting-down, the rotor is subjected to alternating thermal stress, resulting in the fatigue cracks appearing on the metal surface and gradually expand into rotor fracture [16]. In the process of peak regulation, gas-fired unit changes the output dramatically and is in the unstably variable operating condition, which will lead to the deterioration of rotor damage and operating performance, and shortening of unit' service life. As a result, the hidden costs of gas-fired unit such as loss cost and risk cost will increase significantly during peak-regulation, thus increasing the actual cost of peak-regulation. Nevertheless, only gas consumption cost is considered in practical power scheduling and existing peak regulating compensation costs do not take the hidden costs such as the peak-regulation loss into account, which leads to the insufficient willingness of gas-fired unit to provide peak-regulation service [17]. The existing gas-fired unit's peak-regulation compensation mechanism fails to meet the peak-regulation demand of renewable energy-oriented power system. Under this background, the calculation of peak-regulation loss of gas-fired unit can comprehensively reflect the actual peak-regulation cost of gas-fired unit, thereby reducing the number of startup/shutdown times and deep peak-regulation operation time, which can increase the willingness of gas-fired unit to provide peak-regulation service.

Additionally, integrated energy system can break the barrier between different types of energy, thereby giving full play to the coupling and complementary among various energy forms, which is also one of the effective ways to achieve the dual-carbon goal. There are many literatures on the optimization of integrated energy scheduling. In [18], an optimal scheduling model of an energy management system for a hydrogen production system integrated with a photovoltaic system and a storage system is proposed to satisfy the demands of industrial hydrogen facility and maintain reliable operation. Reference [19] proposes a cooperative-game-based day-ahead scheduling model of integrated energy system with shared energy storage. A port integrated energy system optimal scheduling model is proposed in [20], which realizes collaborative optimization of onshore power management and berth allocation. In [21] and [22], a hierarchical stochastic scheduling model based on Stackelberg under uncertain circumstances and a multi-time scale integrated energy system robust optimal scheduling model on the basis of interaction between supply and demand are proposed, respectively. A two-layer scheduling strategy considering dynamic response performance is proposed in [23] in order to rapidly track system's fluctuations. In [24], a two-layer optimization model of community integrated energy system which considers multi-energy demand response and users' satisfaction comprehensively is proposed. Gas-fired units and demand response are respectively viewed as flexibility provisions from supply-side and demand-side, and a flexibility-based maintenance scheduling model of integrated electricity and natural gas system is proposed in [25].

As shown in TABLE 1, existing research has done extraordinary work in the integrated energy scheduling. However, the above researches did not take the peak-regulation effect of gas-fired unit into consideration in integrated energy system optimal scheduling, while considering the peak-regulation of gas-fired unit in integrated electricity and gas system (IEGS) optimal scheduling can promote the consumption of renewable energy. Besides, there is no research studying on the peak-regulation loss of gas-fired unit's rotor in the process of scheduling, and the mechanical damage and economic loss of gas-fired unit are ignored under most conditions. Scheduling strategy aiming at economic objective only will harm the interest and decrease the peak-regulation willingness of gas generator. Therefore, scheduling model ignoring the peak-regulation loss of gas-fired unit does not square with the actual situations. Quantifying the regulation loss and then

TABLE 1. Comparisons of the existing researches.

	[18]	[19]	[20]	[21]	[22]	[23]	[24]	[25]
Hydrogen production	√	×	×	×	×	×	×	×
Renewable energy	√	√	×	×	×	√	×	√
Shared energy storage	×	√	×	×	×	×	×	×
Cooperative game	×	√	√	×	√	×	×	×
Uncertainty	×	×	×	√	√	×	×	√
Hierarchical stochastic	×	×	×	√	×	×	×	×
Robust optimization	×	×	×	×	√	×	×	×
Demand response	×	×	×	×	×	√	√	√
Flexibility	×	×	√	×	×	×	×	√
Gas-fired unit's peak-regulation loss	×	×	×	×	×	×	×	×

calculating the regulation cost respectively for the different stages of gas-fired unit can reduce the deep peak-regulation amount, thus decreasing the wear degree of rotor. Therefore, an optimal scheduling model of IEGS considering gas-fired unit's regulation loss and renewable energy consumption is proposed in this paper, and the major contributions of this paper are presented as follows:

1) The peak-regulation cost models of gas-fired unit under the startup/shutdown mode and variable-load mode are first built for the scheduling of IEGS to estimate gas-fired unit's rotor loss and reflect the actual cost of peak-regulation, thus avoiding unnecessary deep regulation or startup/ shutdown and relieving the rotor loss of peak-regulation.

2) An optimal scheduling model of IEGS considering gas-fired unit's peak-regulation loss is established based on the peak-regulation cost model of gas-fired unit and virtual energy storage model of line-pack, leading to the lower operation cost, higher consumption level of renewable energy, and less carbon emission.

The rest of this paper is organized as follows. In Section II, the rotor loss and whole process cost of gas-fired unit during peak regulating is studied respectively for startup/shutdown mode and variable load mode. Section III establishes an optimal scheduling model of IEGS considering regulation loss of gas-fired unit, aiming at minimize the IEGS operating cost under the constraints of natural gas network, gas-fired unit's peak-regulation and others. A case study is conducted on an IEGS to verify the effectiveness of the proposed model in Section IV. Finally, conclusions are summarized in Section V.

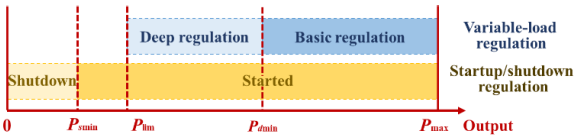

FIGURE 1. Schematic of gas unit peak regulation process.

II. MODELING OF GAS-FIRED UNIT'S PEAK-REGULATION COST CONSIDERING REGULATION LOSS

There are two modes for grid-connected gas-fired unit to participate in peak-regulation, that is, startup/shutdown regulation and variable load regulation, whose processes are shown in FIGURE 1. In FIGURE 1, $P_{\max}$ is the maximum technical output of gas-fired unit, $P_{s\min}$ is the minimum technical output of startup/shutdown peak regulation, $P_{d\min}$ is the minimum technical output of basic regulation, and $P_{\lim}$ is the limit output of deep regulation.

When gas-fired unit operates beyond 50% rated output power, the operation efficiency is higher, gas consumption rate and pollutant emission level are lower and it has secure operation condition and decent technical performances [26]. On the contrary, when gas-fired unit runs below 50% rated output power, as the operating state deviates from the designed condition, the operating performance deteriorates significantly. To be specific, the efficiency of gas-fired unit decreases, the energy loss increases, and the technical property gets worse, resulting in the decline of operation economy, security, and environmental-friendliness. Therefore, 50% rated output power is taken as the critical value of deep regulation and basic regulation.

At present, there are many theoretical analysis and calculation methods for the fatigue characteristics of metal materials. The functions used in the following calculation process have been commonly accepted by the engineering field, and some material constants used in the calculation are usually obtained by experiments and mathematical statistics.

A. STARTUP/SHUTDOWN REGULATION COST OF GAS-FIRED UNIT CONSIDERING REGULATION LOSS

Each startup/shutdown process consumes a certain amount of gas, so the gas consumption cost of start-stop peak-regulation is $C_{\text{ud}} = Vc_{\text{gas}}$, where C_{ud} is the gas consumption cost of gas-fired unit's starting-up or shutting-down, V is the amount of gas consumed in each startup/shutdown process, and c_{gas} is the price of gas.

According to the metal fatigue mechanism, the rotor is subjected to alternating thermal stress in the process of startup and shutdown. Under such alternating stress, fatigue crack will appear on the metal surface and gradually expand to fracture after a certain cycle. Normally, fatigue cracks in rotor firstly occur in the position where the stress is the most concentrated. Therefore, these positions are taken as the calculation object when estimating the loss of rotor.

The thermal stress of gas-fired unit in the startup process is different from that of shutdown process and startup process is always accompanied by heating process, so the change of temperature in the startup/shutdown regulation is nonlinear. Even if it is simplified into a linear process, the thermal cycle processes of starting-up and shutting-down are still asymmetric. The Timo's method [27] is adopted to estimate the regulation loss of rotor, in which the thermal cycle process in starting-up and shutting process are treated as two independent processes, and the regulation loss of starting-up process and shutting-down process are calculated respectively. The average of startup loss and shutdown loss is taken as the regulation loss of each single startup/shutdown regulation.

In order to estimate the regulation loss of gas-fired unit, the yield limit ratio k and the thermal stress concentration coefficient K_{th} of rotor in the process of starting-up and shutting-down are studied first. The yield limit ratio can be obtained through $k = \sigma_{\text{eq}}/\sigma_0$, where σ_{eq} is the nominal equivalent stress of the rotor's shaft at the stress concentration part, and σ_0 is the high temperature yield limit of the rotor's shaft. The thermal stress concentration coefficient can be obtained through $K_{\text{th}} = \sigma_{\max}/\sigma_{\text{eq}}$, where $\sigma_{\max}$ is the maximum stress of elastic groove bottom.

Based on k and K_{th} obtained above, the plastic strain concentration coefficient K_{s} can be obtained by checking the graph of rotor steel plastic strain concentration coefficient [28]. Then the full strain of rotor in the starting-up or shutting-down process can be represented as:

$$\Delta\varepsilon_{\text{t}} = K_{\text{s}}\frac{2\sigma_{\text{eq}}}{E} \tag{1}$$

where E is the elastic modulus of the rotor material.

Then, in order to characterize the fatigue life of metal materials of rotor, the cracking cycle N_{s}^{st} of rotor when starts up or shuts down can be obtained by checking the low-cycle fatigue characteristic curve of rotor's metal material [29]. So the loss rate of a single startup or shutdown process is represented as:

$$d_{\text{s}}^{st} = 1/N_{\text{s}}^{st}, \quad st = \{\text{on,off}\} \tag{2}$$

where the superscript st indicates the startup/shutdown state of gas-fired unit.

Through the above calculations, the loss rate of starting-up and shutting-down process is obtained respectively, whose average is the loss rate of a single startup/shutdown regulation process. Therefore, the economic loss of start-up/shutdown regulation can be expressed by

$$C_{\text{loss}}^{s} = \overline{d}_{\text{s}}S_{\text{g}} = \frac{d_{\text{s}}^{\text{on}} + d_{\text{s}}^{\text{off}}}{2}S_{\text{g}} \tag{3}$$

where S_{g} is the price of gas-fired unit.

To sum up, the whole process cost of gas-fired unit's startup/shutdown peak-regulation can be expressed as follows:

$$C_s = \begin{cases} 0, & P_s = 0 \\ [C_{\text{ud}} + C_{\text{loss}}^{s}]\sum_{t=1}^{T}[T_{s,\text{on}}^{t} + T_{s,\text{off}}^{t}], & P_s \in (0, P_{s\min}] \\ P_s c_{\text{gas}}, & P_s \in (P_{s\min}, P_{\max}] \end{cases} \tag{4}$$

where P_s is the output of gas-fired unit when it participates in startup/shutdown regulation; $T_{s,\text{on}}^{t}$ is the startup binary variable of gas-fired unit, whose value is 1 when gas-fired unit starts up at time t; and $T_{s,\text{off}}^{t}$ is the shutdown binary variable of gas-fired unit, whose value is 1 when gas-fired unit shuts down at time t.

B. THE VARIABLE-LOAD REGULATION COST OF GAS-FIRED UNIT CONSIDERING REGULATION LOSS

In the deep regulation stage, the output of gas-fired unit changes frequently and it is in the low load operation state. Due to the deviation from the designed working condition, the efficiency decline and degree of loss are more serious. Therefore, the rotor loss also exists in the process of variable-load peak-regulation. The calculation of gas-fired unit's variable-load regulation loss is introduced as follows.

The fatigue cracks of rotor generally appear at the stress concentrated parts, which are taken as the rotor loss calculation point. Firstly, the difference between the temperature of calculated point and the average temperature of rotor ΔT_{m} is

$$\Delta T_{\text{m}} = \frac{\eta R^2}{8a} \tag{5}$$

where a is the material temperature conductivity coefficient, η is the temperature rise rate, and R is the radius of rotor.

According to the ΔT_{m} at the calculated point, the stress at the calculated point can be expressed as

$$\sigma_{\text{a}} = E\alpha\Delta T_{\text{m}}/(1-\lambda) \tag{6}$$

where α is the expansion coefficient of rotor material, and λ is the Poisson's ratio.

The Langer formula [30] is used to express the relationship fatigue life and stress of metal materials, which is adopted to calculate the cracking cycle of rotor. Then the loss rate d_{v} of gas-fired unit caused by each deep variable load can be obtained as shown in (7):

$$N_{\text{v}} = \left((\frac{1}{4}E\ln\frac{1}{1-\varphi})/(\sigma_{\text{a}} - \sigma_{\omega})\right)^2 \tag{7}$$

where N_{v} is the cracking cycle of deep variable load regulation, φ is the shrinkage coefficient of material's section, and σ_{ω} is the limit of fatigue strength of material. On this basis, the peak-regulation loss rate of deep variable load regulation can be obtained, which is $d_{\text{v}} = 1/N_{\text{v}}$.

Therefore, the loss cost of gas-fired unit participating in deep variable load regulation is C_{loss}^{d}, which is

$$C_{\text{loss}}^{d} = d_{\text{v}}S_{\text{g}} \tag{8}$$

According to the different stages of variable load regulation of the unit, the whole regulation process cost can be expressed as:

$$C_d = \begin{cases} P_d c_{\text{gas}} & P_{d\,\min} < P_d \le P_{\max} \\ P_d c_{\text{gas}} + C^d_{\text{loss}} & P_{\lim} < P_d \le P_{d\,\min} \end{cases} \tag{9}$$

where P_d is the output of gas-fired unit when participating in deep variable load regulation.

III. SCHEDULING MODEL OF INTEGRATED ELECTRICITY AND GAS SYSTEM CONSIDERING PEAK-REGULATION LOSS

In order to fully consume the renewable energy in IEGS and give play to the peak-regulating effect of gas-fired unit, an optimal scheduling model of IEGS considering the peak-regulation loss and the consumption of renewable energy is established in this paper. The objective function is to minimize the scheduling cost including system operation cost considering regulation loss, renewable energy abandoning penalty, load shedding cost, and emission cost under the constraints of peak regulating, device operation, natural gas network and others. And the steps of the optimization process can be summarized as follows.

STEP 1: Calculate the loss rate and economic loss of gas-fired unit respectively under the startup/shutdown regulation and variable-load regulation mode;
STEP 2: Calculate the whole process cost of gas-fired unit respectively under the startup/shutdown regulation and variable-load regulation mode;
STEP 3: Form the object function of the optimal scheduling model to optimize IEGS total scheduling cost;
STEP 4: Consider the constraints of peak-regulation, natural gas network and other necessary constraints to construct the scheduling model;
STEP 5: Process the optimal model through big-M method, incremental piecewise linearization, and second-order cone relaxation, transforming the model into a mixed integer linear optimization problem;
STEP 6: Initial scenarios of load demand and renewable energy output considering uncertainty are processed by k-means clustering method to reduce the scenario amount;
STEP 7: Scenario analysis method is adopted to process the uncertainty in scheduling;
STEP 8: Use Cplex solver in Yalmip toolbox of Matlab to solve the proposed model;
STEP 9: The optimal scheduling cost and strategy of IEGS are obtained.

A. OBJECTIVE FUNCTION

The scheduling model proposed in this paper takes the lowest total scheduling cost as the objective function including the operation cost considering regulation loss, renewable energy abandoning penalty, load-shedding cost and emission cost, which can be expressed as

$$\min C = C_{\text{ope}} + C_{\text{aban}} + C_{\text{cut}} + C_{\text{carb}} \tag{10}$$

where C is the total scheduling cost; C_{ope} is the operation cost including the energy purchase cost, the peak-regulation cost of gas-fired unit considering regulation loss, and the maintenance cost of gas-fired units, whose expression is shown in (11); C_{aban}, C_{cut} and C_{carb} are the renewable energy abandoning penalty, load-shedding cost and emission cost, whose expressions are shown in (12)-(13), respectively.

$$C_{\text{ope}} = \sum_{t=1}^{T} (c_{\text{gas}} V^t_{\text{pur}} + C_d(P_d) + C_s(P_s) + C_{\text{maint}}) \tag{11}$$

$$C_{\text{aban}} = c_{\text{PV}} \sum_{t=1}^{T} P^t_{\text{PV,wst}} + c_{\text{WT}} \sum_{t=1}^{T} P^t_{\text{WT,wst}} \tag{12}$$

$$C_{\text{cut}} = \sum_{t=1}^{T} P^t_{\text{cut}} c_{\text{cut}} \tag{13}$$

$$C_{\text{carb}} = \sum_{t=1}^{T} (c^{\text{GS}}_{\text{carb}} P^t_{\text{GS}} + c^{\text{CHP}}_{\text{carb}} P^t_{\text{CHP}} + c^{\text{EH}}_{\text{carb}} P^t_{\text{EH}} + c^{\text{P2G}}_{\text{carb}} P^t_{\text{P2G}}) \tag{14}$$

where V^t_{pur} is the total amount of purchased natural gas excluding that consumed by gas-fired unit; $C_d(P_d)$ and $C_s(P_s)$ are the variable load peak-regulation cost and startup/shutdown peak-regulation cost, respectively, which have taken the natural gas consumed in the process of gas-fired unit's power generation into account;C_{maint} is the maintenance cost of gas-fired unit, which is related to the actual output and operation condition of gas-fired unit; c_{PV} and c_{WT} are the penalty cost of per unit photovoltaic and wind turbine power abandoned, respectively; $P^t_{\text{PV,wst}}$ and $P^t_{\text{WT,wst}}$ are abandoned quantity of photovoltaic power and wind turbine power, respectively; P^t_{cut} is the amount of shed load; c_{cut} is the price of per unit load shedding; $c^{\text{GS}}_{\text{carb}}$, $c^{\text{CHP}}_{\text{carb}}$, $c^{\text{EH}}_{\text{carb}}$ and $c^{\text{P2G}}_{\text{carb}}$ are respectively the carbon emission cost for GS, CHP, EH and P2G, as for energy storage device's carbon emission, it's tiny and therefore negligible.

B. CONSTRAINTS

1) CONSTRAINTS OF PEAK-REGULATION

a: UPPER LIMITS OF DEEP VARIABLE LOAD REGULATION

The amount of deep variable load regulation should be under its upper limit:

$$\sum_{t=1}^{T} (P_{d\,\min} - P_d) \le S^{\max}_d \tag{15}$$

where $S^{\max}_d$ is the upper limit of deep variable load regulating capacity of unit d within a day.

b: UPPER LIMITS OF STARTUP/SHUTDOWN PEAK-REGULATION

The number of starting-up and shutting-down within a day should be under its upper limit:

$$\sum_{t=1}^{T} (T^t_{s,\text{on}} + T^t_{s,\text{off}}) \le N^{\max}_s \tag{16}$$

where $N_s^{\max}$ is the upper limit of startup and shutdown times within a day.

c: MINIMUM CONTINUOUS OPERATING TIME AND SHUTDOWN TIME CONSTRAINT

In order to ensure the stable power supply and satisfy the operation requirements of the units, the continuous running time and shutdown time should meet the following constraints:

$$\sum_{t}^{t+T_{\text{on}}^{\min}} T_{s,\text{on}}^{t} \le 1 \tag{17}$$

$$\sum_{t}^{t+T_{\text{off}}^{\min}} T_{s,\text{off}}^{t} \le 1 \tag{18}$$

where $T_{\text{on}}^{\min}$ and $T_{\text{off}}^{\min}$ are the minimum continuous operating time and shutdown time, respectively.

2) CONSTRAINTS OF NATURAL GAS NETWORK CONSIDERING LINE PACK

Natural gas network usually includes natural gas sources, gas storage tank, pressure stations, pipelines, and natural gas loads. The natural gas flows into network from the source and is transmitted to the load through pipelines. In the transmission process, there is pressure loss of natural gas due to the friction resistance in the inner wall of pipeline. In order to transmit natural gas reliably, it is necessary to configure pressure stations in the natural gas network to compensate for the pressure loss [31].

a: NATURAL GAS SOURCE

The natural gas flowing into the network should satisfy the following constraint:

$$S_r^{\min} \le S_r^t \le S_r^{\max} \tag{19}$$

where S_r^t is the natural gas flow of source r at time t; $S_r^{\max}$ and $S_r^{\min}$ are the upper and lower limit of gas source r's gas flow.

b: NATURAL GAS STORAGE TANK

The operation of natural gas storage tank is similar to that of electric energy storage device, whose constraints are shown as follows:

$$0 \le W_{\text{GSS}}^t \le W_{\text{GSS}}^{\max} \tag{20}$$

$$0 \le W_{\text{GSS,in}}^t \le W_{\text{GSS,in}}^{\max} \tag{21}$$

$$0 \le W_{\text{GSS,out}}^t \le W_{\text{GSS,out}}^{\max} \tag{22}$$

$$W_{\text{GSS}}^t = W_{\text{GSS}}^{t-1} + W_{\text{GSS,in}}^t \eta_{\text{GSS}}^{\text{in}} - W_{\text{GSS,out}}^t / \eta_{\text{GSS}}^{\text{out}} \tag{23}$$

$$W_{\text{GSS}}^1 = W_{\text{GSS}}^T \tag{24}$$

where W_{GSS}^t is the natural gas amount stored in tank s at time t; $W_{\text{GSS}}^{\max}$ is the upper limit of storing amount of tank s; $W_{\text{GSS,in}}^t$ and $W_{\text{GSS,out}}^t$ are the stored and released gas of tank s at time t, respectively; $W_{\text{GSS,in}}^{\max}$ and $W_{\text{GSS,out}}^{\max}$ are the upper limits of storing and releasing gas, respectively; $\eta_{\text{GSS}}^{\text{in}}$ and $\eta_{\text{GSS}}^{\text{out}}$ are the storing and releasing efficiency, respectively; and T is the number of scheduling intervals.

c: VIRTUAL ENERGY STORAGE EFFECT OF LINE-PACK

The gas inflow of pipeline at the starting node is different from the outflow at the ending node because of the slow transmission speed and compressible property of natural gas. The difference between the inflow and outflow of the pipeline is stored in the pipeline temporarily, which is defined as line pack [32]. Therefore, line pack is capable of storing gas like the hypostatic gas tank, which can be equivalent to virtual energy storage. The model of line pack is expressed as:

$$M_l^t = M_l^{t-1} + S_{l,\text{in}}^t - S_{l,\text{out}}^t \tag{25}$$

where M_l^t is the line pack of pipeline l at time t; $S_{l,\text{in}}^t$ and $S_{l,\text{out}}^t$ are the inflow and outflow of pipeline l, respectively, which satisfy the Weymouth steady flow equation [33], that is, the gas flow in pipeline and the pressure at the both ends of pipeline satisfy the following constraint:

$$(S_{l,\text{in}}^t + S_{l,\text{out}}^t)\left|S_{l,\text{in}}^t + S_{l,\text{out}}^t\right|/4 = \Phi_l[(p_{l,\text{in}}^t)^2 - (p_{l,\text{out}}^t)^2] \tag{26}$$

Equation (26) is non-convex and nonlinear, which is difficult to solve by commercial solver. Therefore, incremental piecewise linearization [33] is adopted to linearize the left part of (26), which can be substitute by (27)-(30) after processing.

$$\widetilde{S_{l,1}^t}\left|\widetilde{S_{l,1}^t}\right| + \sum_{z=1}^{Z-1}(\widetilde{S_{l,z+1}^t}\left|\widetilde{S_{l,z+1}^t}\right| - \widetilde{S_{l,z}^t}\left|\widetilde{S_{l,z}^t}\right|)\delta_{l,z}^t = 4\Phi_l(\Pi_{l,\text{in}}^t - \Pi_{l,\text{out}}^t) \tag{27}$$

$$\widetilde{S_l^t} = \widetilde{S_{l,1}} + \sum_{z=1}^{Z-1}(\widetilde{S_{l,z+1}^t} - \widetilde{S_{l,z}^t})\delta_{l,z}^t \tag{28}$$

$$\delta_{l,z+1}^t \le \theta_{l,z}^t \le \delta_{l,z}^t \tag{29}$$

$$0 \le \delta_{l,z}^t \le 1 \tag{30}$$

where z stands for the piecewise interval where the discrete point locates, $z = 1, 2, \ldots, Z$, which means there are Z-1 piecewise intervals and Z discrete points, Replacing the squared gas pressure with a single variable as a whole, $\Pi_{l,\text{in}}^t = (p_{l,\text{in}}^t)^2$; S_l^t is the average of the pressure at both ends of pipeline l, $S_l^t = \left[S_{l,\text{in}}^t + S_{l,\text{out}}^t\right]/2$; $\delta_{l,z}^t$ is a continuous variable whose value ranges from 0 to 1, which is used to represent the position of the discrete point on the z^{th} piecewise interval; $\theta_{l,z}^t$ is an auxiliary binary variable, whose function is to ensure the entire piecewise intervals are filled continuously from left to right through (29).

d: PRESSURE STATION AND COMPRESSOR

The main component of a pressure station is the compressor. The energy consumed by the compressor is generally considered to come from the natural gas flowing through

it, so the compressor can be regarded as a natural gas load [34]. The amount of natural gas consumed by the compressor is determined by the flow rate of the natural gas passing through it and compression ratio, whose energy consumption expression is non-convex and nonlinear. As for the natural gas consumed by compressor is subtle and not the key of this paper, linear approximate substitution method is adopted to simplify the model of compressor. The model of compressor is

$$S_q^{\min} \le S_q^t \le S_q^{\max} \tag{31}$$

$$\xi_q^t = K_q S_q^t \tag{32}$$

$$(k_q^{\min})^2 \le \frac{\prod_{q,\text{out}}^t}{\prod_{q,\text{in}}^t} \le (k_q^{\max})^2 \tag{33}$$

where S_q^t is the gas flow of compressor q at time t; $S_q^{\max}$ and $S_q^{\min}$ are respectively the upper and lower limits of the gas flow allowed to flow through the compressor; ζ_q^t is the gas flow consumed by compressor q at time t; K_q is the gas consumption coefficient; $k_q^{\max}$ and $k_q^{\min}$ are respectively the upper and lower limits of compression ratio, respectively; in order to be consistent with the linearization process of (26), $\prod_{q,\text{out}}^t$ and $\prod_{q,\text{in}}^t$ are respectively the squared outflow and inflow gas pressure of compressor q at time t, that is, $\Pi_{q,\text{out}}^t = (p_{q,\text{out}}^t)^2$ and $\Pi_{q,\text{in}}^t = (p_{q,\text{in}}^t)^2$.

e: NODE PRESSURE OF NATURAL GAS NETWORK

All node pressure in the natural gas network should meet the upper and lower limits. In addition, the node pressure is still expressed in its squared term in order to be consistent with the linearization process of (26). Thus, the node pressure should satisfy the following constraint:

$$\Pi_j^{\min} \le \Pi_j^t \le \Pi_j^{\max} \tag{34}$$

where Π_j^t is the squared node pressure of node j, $\Pi_j^t = (p_j^t)^2$; $\Pi_j^{\min}$ and $\Pi_j^{\max}$ are the lower and upper limits of squared node pressure of node j, respectively.

3) CONSTRAINTS OF DEVICE OPERATION

a: COMBINED HEAT AND POWER (CHP) UNIT

CHP converts natural gas into heat and electricity, and the operating mode is 'power by heat', thus the electric output is determined by the heat demand of CHP. The operation of CHP can be expressed as (35)-(38), among which (35) indicates the gas-heat conversion, (35) indicates the power-heat conversion, and (36)-(37) are respectively the upper and lower limits for heat output and climbing rate.

$$H_{\text{CHP}}^t = \eta_{\text{CHP}}^{\text{G-H}} G_{\text{CHP}}^t \tag{35}$$

$$P_{\text{CHP}}^t = H_{\text{CHP}}^t / \eta_{\text{CHP}}^{\text{H-E}} \tag{36}$$

$$H_{\text{CHP}}^{\min} \le H_{\text{CHP}}^t \le H_{\text{CHP}}^{\max} \tag{37}$$

$$\left| P_{\text{CHP}}^{t+1} - P_{\text{CHP}}^t \right| \le U_{\text{CHP}}^{\max} \tag{38}$$

where P_{CHP}^t, H_{CHP}^t and G_{CHP}^t are the electric output, thermal output and natural gas power of CHP unit, respectively; $\eta_{\text{CHP}}^{\text{G-H}}$ and $\eta_{\text{CHP}}^{\text{H-E}}$ are the natural gas-heat conversion efficiency and the heat-electric conversion efficiency of CHP unit, respectively; and $U_{\text{CHP}}^{\max}$ is the upper limit of the climbing rate of CHP unit. It should be noted the 'power by heat' operating mode shown in (39) makes CHP's electric output lack of flexibility and therefore cannot act as a peaking power resource.

b: GAS-FIRED UNIT

$$P_{\text{GS}}^t = \eta_{\text{GS}} G_{\text{GS}}^t \tag{39}$$

$$\begin{cases} P_a \le P_{\text{GS},d}^t \le P_{GS}^{\max} \\ P_{s\min} U_s^t \le P_{\text{GS},s}^t \le P_{\text{GS}}^{\max} U_s^t \end{cases} \tag{40}$$

$$\left| P_{\text{GS}}^{t+1} - P_{\text{GS}}^t \right| \le U_{\text{GS}}^{\max} \tag{41}$$

where P_{GS}^t and G_{GS}^t are the electric output power and natural gas input power of gas-fired unit, respectively; s stands for the startup/shutdown peak-regulation unit and d stands for the variable load peak-regulation unit; U_s^t is the binary variable of unit s at time t, whose value is 1 when the unit is in operation and 0 otherwise; and $U_{\text{GS}}^{\max}$ is the upper limit of the ramping rate of the unit.

c: ELECTRICAL BOILER (EB)

$$H_{\text{EB}}^t = \eta_{\text{EB}} P_{\text{EB}}^t \tag{42}$$

$$H_{\text{EB}}^{\min} \le H_{\text{EB}}^t \le H_{\text{EB}}^{\max} \tag{43}$$

$$\left| H_{\text{EB}}^{t+1} - H_{\text{EB}}^t \right| \le U_{\text{EB}}^{\max} \tag{44}$$

where H_{EB}^t and P_{EB}^t are the heating power and electric power of EB, respectively; $H_{\text{EB}}^{\max}$ and $H_{\text{EB}}^{\min}$ are the upper and lower limits of heating output power; and $U_{\text{EB}}^{\max}$ is the upper limit of EB's climbing rate.

d: POWER TO GAS (P2G)

Power to gas (P2G) converts excess electric power into natural gas for use of gas loads and gas-consuming devices, which is conductive to promoting the consumption of renewable energy. The operation constraints of P2G are as follows:

$$P_{\text{P2G}}^{\min} \le P_{\text{P2G}}^t \le P_{\text{P2G}}^{\max} \tag{45}$$

$$G_{\text{P2G}}^t = P_{\text{P2G}}^t \eta_{\text{P2G}} \tag{46}$$

where P_{P2G}^t and G_{P2G}^t are the electric power and natural gas output of P2G, respectively; $P_{\text{P2G}}^{\max}$ and $P_{\text{P2G}}^{\min}$ are the upper and lower limits of P2G's electric power.

e: ENERGY STORAGE DEVICE

Energy storage devices (ESDs) should satisfy the constraints of stage of charge (SOC) shown in (48)-(49), whose definition is shown in (47). The charging and discharging power should satisfy the constraints shown in (50)-(51). ESDs can not charge and discharge at the same time, whose corresponding

constraint is expressed as (52).

$$S^t = (1-\gamma^{\text{los}})S^{t-1} + (\gamma^{\text{cha}}P^t_{\text{cha}} - \frac{P^t_{\text{dis}}}{\gamma^{\text{dis}}})\Delta t \tag{47}$$

$$\gamma_{\min}M_{\text{ES}} \le S^t \le \gamma_{\max}M_{\text{ES}} \tag{48}$$

$$S^0 = S^T \tag{49}$$

$$0 \le P^t_{\text{cha}} \le P^{\max}_{\text{cha}}B^t_{\text{cha}} \tag{50}$$

$$0 \le P^t_{\text{dis}} \le P^{\max}_{\text{dis}}B^t_{\text{dis}} \tag{51}$$

$$B^t_{\text{cha}} + B^t_{\text{dis}} \le 1 \tag{52}$$

where S^t is the SOC value of ESDs at time t; γ^{los}, γ^{cha} and γ^{dis} are the energy loss coefficient, charging efficiency and discharging efficiency of ESDs, respectively; Δt is the scheduling time interval of ESDs; M_{ES} is the total capacity of the constructed ESDs; P^t_{cha} and P^t_{dis} are the charging power and discharging power of ESDs, respectively; $\gamma_{\max}$ and $\gamma_{\min}$ are respectively the proportions of upper and lower SOC in ESDs' total capacity; $P^{\max}_{\text{cha}}$ and $P^{\max}_{\text{dis}}$ are the upper limits of charging and discharging power, respectively; B^t_{cha} and B^t_{dis} are the auxiliary binary variables of charging/ discharging at time t.

4) CONSTRAINTS OF POWER BALANCE

The electrical power, thermal power, and natural gas flow of IEGS should maintain balance between the supply and demand, whose expressions are shown as follows:

$$\begin{aligned} &A_{\text{CHP},c}P^t_{\text{CHP},c} + A_{\text{GS},g}P^t_{\text{GS},g} + A_{\text{P2G},k}A^t_{\text{P2G},k} + A_{\text{ES,e}}P^t_{\text{e,dis}} \\ &\quad + A_{\text{PV},v}P^{\text{use},t}_{\text{PV},v} + A_{\text{WT},w}P^{\text{use},t}_{\text{WT},w} \\ &= P^t_{\text{load},i} + A_{\text{EH},h}P^t_{\text{EH},h} + A_{\text{ES,s}}P^t_{\text{s,cha}} - P^t_{\text{cut},i} \end{aligned} \tag{53}$$

$$A_{\text{EH},h}H^t_{\text{EH},h} + A_{\text{CHP},c}H^t_{\text{CHP},c} = H^t_{\text{load},i} - H^t_{\text{cut},i} \tag{54}$$

$$\begin{aligned} &B_{\text{CHP},c}G^t_{\text{CHP},c} + B_{\text{GS},g}G^t_{\text{GS},g} + B_{\text{GSS},u}W^{\text{in},t}_{\text{GSS},u} \\ &\quad + B_{\text{CP},q}\xi^t_q + G^t_{\text{load},j} \\ &= B_l S^t_l + B_{\text{GSS},u}W^{\text{out},t}_{\text{GSS},u} + B_{\text{P2G},k}G^t_{\text{P2G},k} + B_r S^t_r \end{aligned} \tag{55}$$

where $A_{\text{CHP},c}$ is the element of the association matrix of CHP unit and power system's nodes, whose value is 1 when the corresponding node is equipped with CHP and 0 otherwise; $A_{\text{GS},g}, A_{\text{P2G},k}, A_{\text{ES},e}, A_{\text{PV},v}, A_{\text{WT},w}$ and $A_{\text{EH},h}$ are respectively the association matrix of gas-fired unit, P2G, ESDs, photovoltaic, wind turbine and electric boiler with power system's nodes, whose value rules are the same as $A_{\text{CHP},c}$; $B_{\text{CHP},c}$, $B_{\text{GS},g}$, $B_{\text{GSS},u}$, $B_{\text{CP},q}$, $B_{\text{P2G},k}$ and B_r are respectively the value of association matrix of CHP, gas-fired unit, gas tank, compressor, P2G and gas source with natural gas network, whose value rules are also the same as $A_{\text{CHP},c}$; B_l is the element of association matrix of pipeline, whose value is 1 when the current node is the injection node, -1 when the current node is the outflow node, and 0 when the node is disconnected to the pipeline.

Besides, the DistFlow based power flow model [35] is adopted in this paper to constrain the power flow in the power network. This part is similar with the conventional scheduling of power system, which will not be introduced in detail here.

In order to solve the above IEGS optimal scheduling model, big-M method is used to process the piecewise function in (4) and (9). Besides, incremental piecewise linearization is adopted to linearize the nonlinear (26) and second-order cone relaxation is used to relax the non-convex constraints of power flow, through which the proposed model is transformed into a mixed integer linear optimization problem.

It has to be mentioned that there is a great uncertainty existing in load demand and the output of renewable energy, thus the optimal scheduling strategy in a single scene probably is unable to adapt to most conditions, which is against the security and stability of the system. In order to cope with the uncertainty in IEGS scheduling, scenario analysis (SA) is adopted to load uncertainty and random fluctuations of renewable energy's output. However, a large quantity of scenarios will cause an enormous burden on computation. In order to cope with the excessive computation amount and time, k-means clustering method is adopted to reduce the scenario amount and obtain the optimal typical scenario set.

Eventually, the Yalmip toolbox of Matlab is used to invoke Cplex solver to solve the proposed model on the optimal typical scenario set, and then the optimal scheduling cost and strategy of IEGS considering uncertainty are obtained.

IV. CASE STUDY

In order to verify the effectiveness of the proposed IEGS optimal scheduling model considering peak-regulation loss and renewable energy consumption, a modified IEGS with a high proportion of renewable energy from Guangdong province, China is taken as an example to conduct the case study, which consists of a 28-node power network and a 20-node natural gas network. The initial load and renewable energy output are generated randomly to simulate the uncertainty and fluctuation, which are shown in Appendix. The optimal typical scenario set, to be specific, the curves of load demand and renewable energy output are shown in FIGURE 2.

To better demonstrate the effectiveness and priority of the proposed model in IEGS scheduling, the following models are set in this paper for comparative analysis: the proposed IEGS scheduling model considering peak-regulation loss (M-PRL), an IEGS scheduling model that does not take the peak-regulation loss into account when using gas-fired unit as a peak-regulation resource (M-nPRL), and an IEGS scheduling model that does not regard gas-fired unit as a peak-regulation resource (M-nPR).

Cplex solver is used to solve the above model and then the optimal scheduling strategy and scheduling costs of IEGS are obtained, as shown in FIGURE 3 and TABLE 2, respectively. It can be observed from TABLE 2 that the total scheduling cost of M-PRL is ¥ 123.18 million, which is 7.11% and 2.49% lower than those of M-nPRL and M-nPR, respectively. To be specific, the generating cost of gas-fired unit in M-PRL is ¥ 54.42 million, while the gas-fired unit's generating cost in M-nPRL and M-nPR are respectively ¥ 63.47 million and ¥ 56.42 million, that is, the generating cost of gas-fired unit in M-PRL is respectively ¥ 9.05 million and

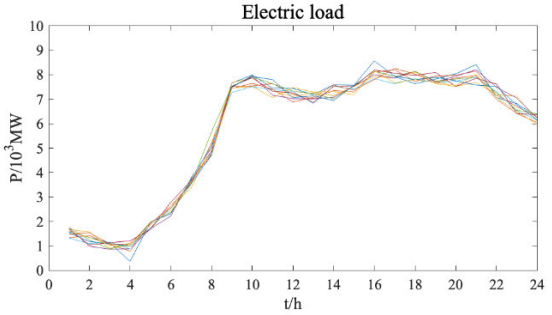

(a) Optimal typical scenario set of electric load

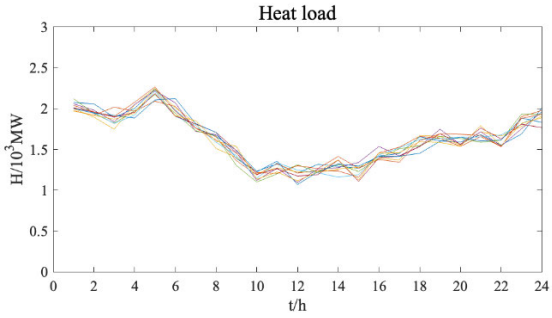

(b) Optimal typical scenario set of heat load

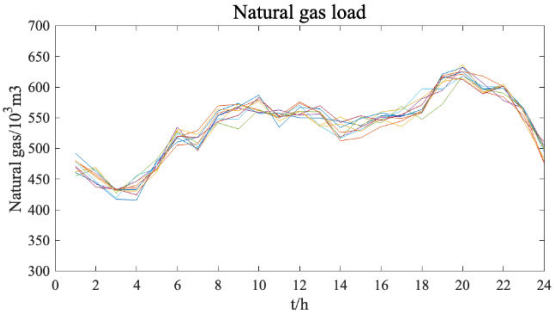

(c) Optimal typical scenario set of natural gas load

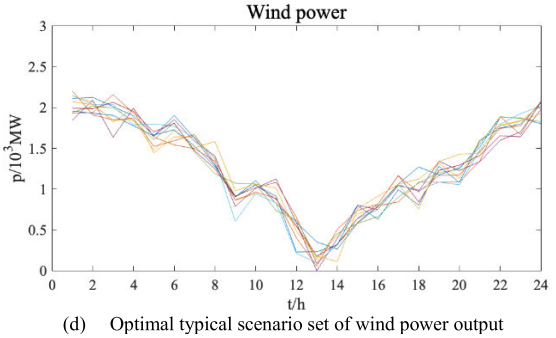

(d) Optimal typical scenario set of wind power output

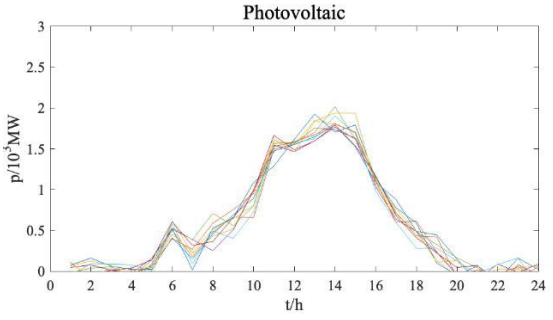

(e) Optimal typical scenario set of photovoltaic output

FIGURE 2. Optimal typical scenario set of load curves and renewable energy output.

TABLE 2. The comparisons of scheduling costs of M-PRL, M-nPRL and M-nPR.

Cost/ million (￥)	M-PRL	M-nPRL	M-nPR
Generating cost of gas-fired unit	54.42	63.47	56.42
Energy purchasing cost	45.38	45.58	45.60
Renewable energy abandoning penalty	2.76	2.83	3.12
Load-shedding cost	0.03	0.03	0.03
Emission cost	20.58	20.70	21.15
Total cost	123.18	132.61	126.33

TABLE 3. The comparisons of environmental effects of the scheduling results of M-PRL, M-nPRL and M-nPR.

Model	Carbon emission/t	Renewable energy consumption ratio
M-PRL	113.22	95.03%
M-nPRL	113.32	94.91%
M-nPR	115.53	94.38%

￥ 2 million lower than that of M-nPRL and M-nPR. This is because peak-regulation loss is considered in M-PRL (the regulation loss rate obtained through the method in this paper of startup/shutdown regulation and variable-load regulation are respectively 0.025% and 0.0006%) and thus relieving the tear of the unit's rotor and the maintenance cost of gas-fired unit is included in the generating cost, considering the peak-regulation loss effectively reduces the maintenance cost and therefore the generating cost of gas-fired unit and therefore the generating cost of M-PRL is obviously lower than that of M-nPRL. Besides, gas-fired unit in M-nPR do not participate in the peak-regulation, so its maintenance cost and generating cost of gas-fired unit is lower than that of M-nPRL. It is worth mentioning that considering the regulation loss will effectively reduce the maintenance cost when participating in peak-regulation, which will effectively bring about the higher willingness of gas generator to provide peak-regulation service. The renewable energy abandoning penalty of M-PRL, M-nPRL, and M-nPR are respectively ￥ 2.76 million, ￥ 2.83 million, and ￥ 3.12 million, which is because the strong ramping ability and peak-regulation effect of gas-fired unit can effectively cope with the volatility and uncertainty of renewable energy output, thus reducing the abandoned renewable energy power in M-PRL and M-nPRL and the corresponding abandoning penalty, while in M-nPR the peaking effect of gas-fired unit is ignored and therefore increase the penalty. There is no significant difference found in the load shedding cost of the three models, which are all ￥ 0.03 million. Additionally, the carbon emission cost of M-PRL is the lowest in the three models, which is ￥ 20.58 million and is 0.58% and 2.7% lower than that of M-nPRL and M-nPR. This is due to the output of gas-fired unit can be adjusted quickly to satisfy the supply-demand balance of IEGS when the output of renewable energy changes dramatically, thus reducing the emission amount of the system in M-PRL and M-nPRL.

The environmental benefits of the three models' scheduling results are shown in TABLE 3. It can be seen from TABLE 3 that the carbon emission of M-PRL is 113.22t, which is the lowest in the three models, while the carbon

emission of M-nPRL and M-nPR are respectively 113.32t and 115.53t. Meanwhile, the renewable energy consumption ratio of M-PRL, M-nPRL, and M-nPR are respectively 95.03%, 94.91%, and 94.38%. The reason why the consumption ratio in M-PRL and M-nPRL are higher is that gas-fired unit can rapidly reduce its output when the output of renewable energy is high and increase its output when the output of renewable energy is low, so as to promote the consumption of renewable energy and reduce carbon emission. However, the high gas-fired unit's maintenance cost of peak-regulation in M-nPRL decrease the willingness of gas generator to provide regulation service, so that the consumption of M-nPRL is slightly lower than that of M-PRL. It can be concluded that peak-regulation effect of gas-fired unit leads to the higher renewable energy consumption level and lower carbon emission while maximally fulfilling the demand of IEGS.

Combining TABLE 2 and TABLE 3, it can be concluded that the comprehensive economic and environmental benefits of M-PRL is the best in the compared models. It can realize a lower carbon emission and higher renewable energy consumption while reducing the scheduling cost, which proves the superiority of the proposed model.

From the scheduling strategies of IEGS shown in FIGURE 3, when the load demand is low while the output of wind turbine is high during night (23:00-4:00), excess wind turbine power is stored by ESD or converted into natural gas through P2G to help consume the redundant wind power. Besides, the outputs of gas-fired units remains low to provide more space to consume wind turbine power. From this point, both ESD and gas-fired unit can play a significant role in the promotion of renewable energy. Furthermore, the load demand is quite high during 9:00-12:00, so ESD discharges to satisfy the load. ESD is definitely a great peaking resource, however, the installed capacity of ESD is commonly low thus restricting its peak-regulation effect. To deal with the extra natural gas caused by gas supply-demand imbalance, natural gas stored in gas pipeline through line-pack increases at 2:00, 3:00, 9:00, 10:00, et al., which equivalently serves as virtual energy storage. It can be concluded that P2G and line-pack cooperating with gas-fired units can effectively improve the consumption of renewable energy in IEGS. Besides, during the periods of high photovoltaic output at noon (e.g. 9:00-11:00), the output of gas-fired unit decreases rapidly. And in the following periods, the output of photovoltaic decreases and the output of gas-fired unit correspondingly increases to satisfy the demand of power system, giving full play to the peak-regulation characteristics of gas-fired unit. Specifically, it can be seen from the renewable energy output curve in FIGURE 2 that the output of photovoltaic decreases rapidly from 2200 MW to 1325 MW at 16:00. Combined with the electric power scheduling strategy in FIGURE 3, it can be observed that the output of gas-fired unit increases rapidly at this time. In addition, it can be seen from FIGURE 3, the gas stored in line-pack releases for the use of gas-fired unit (e.g.: 13:00-17:00), and natural gas flows into pipeline and the line-pack increases when the output of renewable energy

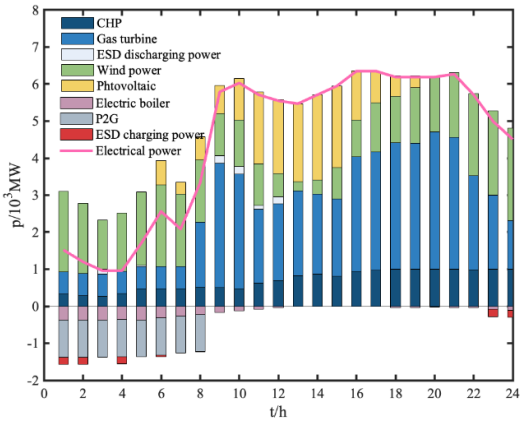

(a) The optimal scheduling strategies of electric power in IEGS

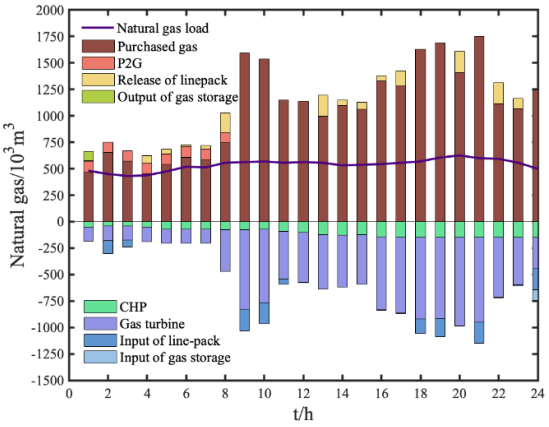

(b) The optimal scheduling strategies of natural gas in IEGS

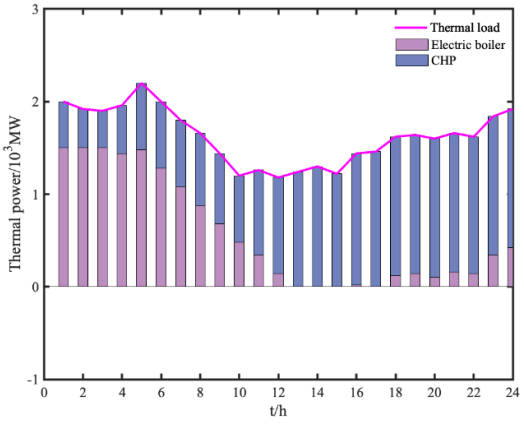

(c) The optimal scheduling strategies of heating power in IEGS

FIGURE 3. The optimal scheduling strategies of electric, natural gas and heating power.

increases (e.g. 9:00 and 10:00). It can be concluded that the gas line-pack cooperates with gas-fired unit to play a significant role in peak-regulation and promote the consumption of renewable energy.

In order to better demonstrate the effect of regulation loss on the scheduling results, the output of M-PRL and M-nPRL

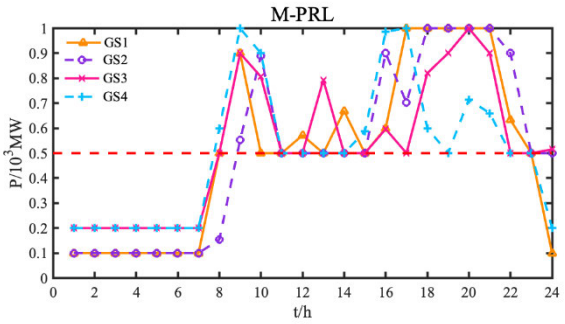

(a) The output curves of gas generators with the rotor loss of peak regulation taken into account

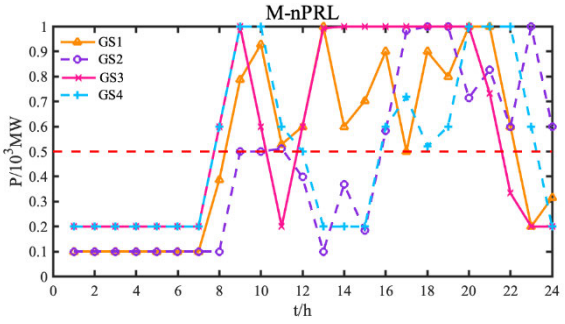

(b) The output curves of gas generators ignoring the rotor loss of peak regulation

FIGURE 4. The output curves of gas generators.

TABLE 4. Scheduling results comparisons under different renewable energy penetration.

Penetration percentage /%		Scheduling cost /million (￥)	Renewable energy consumption /%	Carbon emission /t
100	M-PRL	123.18	95.03	113.22
	M-nPR	126.33	94.38	115.53
95	M-PRL	125.18	95.69	115.14
	M-nPR	128.41	95.20	117.64
90	M-PRL	127.19	96.42	116.95
	M-nPR	130.57	95.84	119.75
85	M-PRL	128.43	97.22	118.8
	M-nPR	132.75	96.71	121.85
80	M-PRL	130.83	97.54	121.06
	M-nPR	134.92	97.70	123.95
75	M-PRL	133.24	99.12	122.37
	M-nPR	137.11	97.35	126.17
70	M-PRL	135.54	99.64	124.39
	M-nPR	139.62	99.36	128.17

TABLE 5. Scheduling results comparisons under different ESD capacity.

ESD capacity percentage/ %	Scheduling cost /million (￥)	Renewable energy consumption /%	Carbon emission /t
100	123.18	95.03	113.22
90	123.30	94.94	113.27
80	123.41	94.86	113.32
70	123.53	94.78	113.37
60	123.64	94.69	113.42

are compared and the output curves of gas-fired units in the above two models are shown in FIGURE 4. From FIGURE 4, it can be seen that the output of gas-fired units changes rapidly in both models in order to cope with the volatility and uncertainty of renewable energy. Nevertheless, it can be observed that there are more periods in M-nPRL that the output of gas-fired units is below 50% rated output power. Apart from the periods in common (0:00-8:00) that output of gas-fired unit in both M-PRL and M-nPRL are below 50% rated output power, the output of gas-fired unit in M-nPRL is below 50% rated output power during 11:00-15:00, and 22:00-23:00. And the deep regulation amount (the differences between the actual output and 50% rated output power when the output is below 50% rated output power) of M-nPRL is 11.63% more than that of M-PRL, which is also obviously less than that of M-nPRL. And in M-PRL, the period that gas-fired unit's output is below 50% is shorter than that of M-nPRL. Apart from the difference in variable-load regulation, the effect of startup/shutdown regulation is also obvious, to be specific, all the gas-fired units in M-PRL startup/ shutdown no more than a single time, while GS2 in M-nPRL starup/ shutdown twice. Therefore, IEGS scheduling strategy considering peak-regulation loss could achieve less conditions that gas-fired unit operates below 50% rated output power or less startup/ shutdown times. In this way, the wear caused by peak-regulation can be relieved and a longer service life of gas-fired unit can be obtained.

As for the building of renewable energy oriented power system is a long-term project, the scheduling results of M-PRL and M-nPRL are compared under different penetration of renewable energy, which is shown in TABLE 4. The 100% penetration percentage in TABLE 4 is equal to the renewable energy capacity of the previous analysis shown in TABLE 3. It can be observed that under every penetration percentage, the scheduling cost of M-PRL is lower than M-nPR, the renewable energy consumption is higher than M-nPR, and the carbon emission is less than M-nPR. This is because gas-fired unit in M-PRL can plays a role in peak-regulation thus promoting the consumption of renewable energy. Besides, the increase of scheduling cost, renewable energy and carbon emission of both models occur along with the decrease of renewable energy penetration percentage. This means the larger renewable energy penetration leads to the greater obstacle to the consumption. And the comparisons further demonstrate gas-fired unit's effect in peaking and promoting renewable energy consumption.

In addition to gas-fired unit, ESD can also play a role in peak-regulation. So the scheduling results of M-PRL under different ESD capacity is also compared, as is shown in TABLE 5, in which the 100% ESD capacity percentage is equal to the capacity of M-PRL shown in TABLE 3. It can be seen from TABLE 5 that the scheduling cost and carbon emission increases and the renewable energy consumption decreases along with the reduction of ESD capacity. And the results indicate that ESD is a significant regulation resource, and it can bring economic and environmental benefits coordinating with gas-fired units.

To sum up, the optimal IEGS scheduling model proposed in this paper considering gas-fired unit's peak-regulation loss

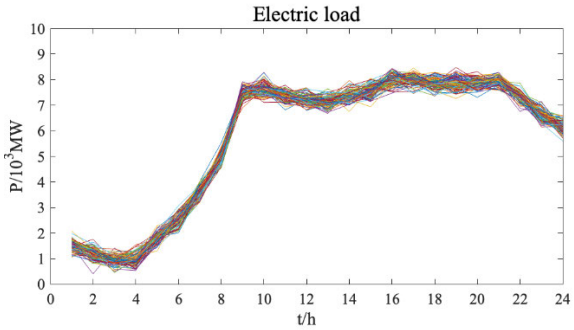

FIGURE 5. Scenarios of electric load considering uncertainty.

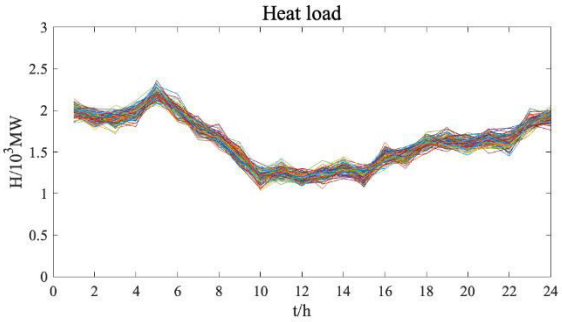

FIGURE 6. Scenarios of heat load considering uncertainty.

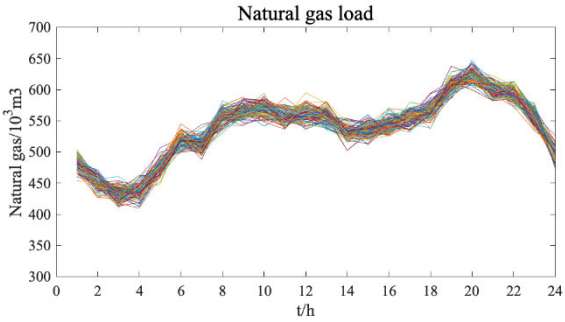

FIGURE 7. Scenarios of natural gas load considering uncertainty.

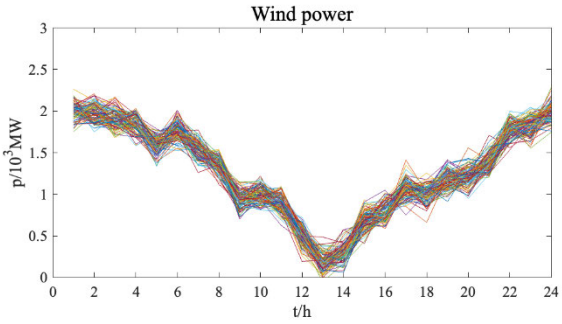

FIGURE 8. Scenarios of wind power output considering uncertainty.

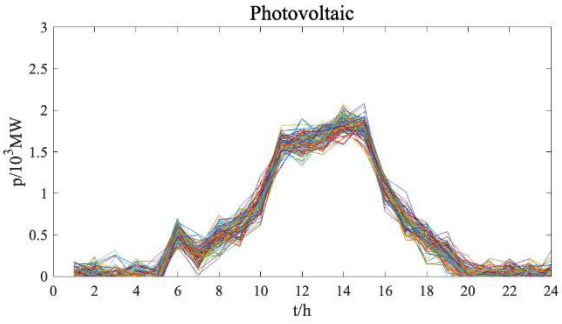

FIGURE 9. Scenarios of photovoltaic output considering uncertainty.

can promote the consumption of renewable energy and reduce the scheduling cost at the same time. It can adapt to the uncertainty and volatility, which improves the consumption of renewable energy and reduces the carbon emissions of the system, thus helping realize the goal of ''dual-carbon''.

V. CONCLUSION

The peak-regulation cost models of gas-fired unit under the startup-shutdown mode and variable-load mode are first built, and then an optimal scheduling model of IEGS considering gas-fired unit's peak-regulation loss is established based on the peak-regulation cost model of gas-fired unit and virtual energy storage model of line-pack. And scenario analysis method is adopted to cope with the uncertainty of load demand and renewable energy output in the scheduling process. The case study on a modified IEGS from Guangdong province, China demonstrates that less scheduling cost and less shed loads of IEGS are obtained by the proposed model considering peak-regulation characteristics of gas-fired unit; the higher consumption level of renewable energy and the less carbon emission are achieved by the proposed model due to the peak-regulation ability and the cooperation with virtual energy storage of gas-fired unit. It can also be concluded that, as for the gas-fired units, their economic profit could be increased and therefore the stronger willingness to provide peak-regulation service could be realized by considering the hidden cost of peak-regulation loss; besides, less operation time of gas-fired unit in the stage of deep peak-regulation and less startup/shutdown times could be obtained in the proposed model, in this way, the rotor wear degree is effectively relieved and the operation performance and security of gas-fired unit are improved. Besides, it can be concluded that the larger renewable energy penetration also brings about the bigger difficulty in the consumption.

APPENDIX

The initial scenarios of electric, heat, natural gas load, and the output of renewable energy considering the uncertainty are shown in FIGURES 5–9.

REFERENCES

[1] W. Shen, J. Qiu, K. Meng, X. Chen, and Z. Y. Dong, "Low-carbon electricity network transition considering retirement of aging coal generators," *IEEE Trans. Power Syst.*, vol. 35, no. 6, pp. 4193–4205, Nov. 2020. [Online]. Available: https://ieeexplore.ieee.org/document/9096534

[2] Y. Wang, H. Chen, B. Gao, X. Xiao, R. Torquato, and F. C. L. Trindade, "Harmonic resonance analysis in high-renewable-energy-penetrated power systems considering frequency coupling," *Energy Convers. Econ.*, vol. 3, no. 5, pp. 333–344, Oct. 2022, doi: 10.1049/enc2.12068.

[3] C. Chen, H. Liang, X. Zhai, J. Zhang, S. Liu, Z. Lin, and L. Yang, "Review of restoration technology for renewable-dominated electric power systems," *Energy Convers. Econ.*, vol. 3, no. 5, pp. 287–303, Oct. 2022, doi: 10.1049/enc2.12064.

[4] R. M. Elavarasan, G. M. Shafiullah, S. Padmanaban, N. M. Kumar, A. Annam, A. M. Vetrichelvan, L. Mihet-Popa, and J. B. Holm-Nielsen, "A comprehensive review on renewable energy development, challenges, and policies of leading Indian states with an international perspective," *IEEE Access*, vol. 8, pp. 74432–74457, 2020. [Online]. Available: https://ieeexplore.ieee.org/document/9072152

[5] A. Khosravani, E. Safaei, M. Reynolds, K. E. Kelly, and K. M. Powell, "Challenges of reaching high renewable fractions in hybrid renewable energy systems," *Energy Rep.*, vol. 9, pp. 1000–1017, Dec. 2023. [Online]. Available: https://www.webofscience.com/wos/alldb/full-record/WOS:000904823100008

[6] E. Du, N. Zhang, B.-M. Hodge, Q. Wang, C. Kang, B. Kroposki, and Q. Xia, "The role of concentrating solar power toward high renewable energy penetrated power systems," *IEEE Trans. Power Syst.*, vol. 33, no. 6, pp. 6630–6641, Nov. 2018. [Online]. Available: https://ieeexplore.ieee.org/document/8356090

[7] B. Yang, B. Liu, H. Zhou, J. Wang, W. Yao, S. Wu, H. Shu, and Y. Ren, "A critical survey of technologies of large offshore wind farm integration: Summary, advances, and perspectives," *Protection Control Modern Power Syst.*, vol. 7, no. 1, p. 17, Dec. 2022. [Online]. Available: https://www.webofscience.com/wos/alldb/full-record/WOS:000789150100001WOS:000789150100001

[8] S. Liu, C. Zhou, H. Guo, Q. Shi, T. E. Song, I. Schomer, and Y. Liu, "Operational optimization of a building-level integrated energy system considering additional potential benefits of energy storage," *Protection Control Modern Power Syst.*, vol. 6, no. 1, pp. 1–10, Dec. 2021. [Online]. Available: https://www.webofscience.com/wos/alldb/full-record/WOS:000621949200002

[9] W. Wang, S. Huang, G. Zhang, J. Liu, and Z. Chen, "Optimal operation of an integrated electricity-heat energy system considering flexible resources dispatch for renewable integration," *J. Modern Power Syst. Clean Energy*, vol. 9, no. 4, pp. 699–710, Jul. 2021. [Online]. Available: https://ieeexplore.ieee.org/document/9502595

[10] L. Yang, N. Zhou, G. Zhou, Y. Chi, N. Chen, L. Wang, Q. Wang, and D. Chang, "Day-ahead optimal dispatch model for coupled system considering ladder-type ramping rate and flexible spinning reserve of thermal power units," *J. Modern Power Syst. Clean Energy*, vol. 10, no. 6, pp. 1482–1493, 2022. [Online]. Available: https://ieeexplore.ieee.org/document/9831173

[11] M. J. E. Alam, K. M. Muttaqi, and D. Sutanto, "A controllable local peak-shaving strategy for effective utilization of PEV battery capacity for distribution network support," *IEEE Trans. Ind. Appl.*, vol. 51, no. 3, pp. 2030–2037, May 2015. [Online]. Available: https://ieeexplore.ieee.org/document/6954490

[12] G. Wang, M. Bi, H. Fan, Y. Fan, C. Huang, Y. Shi, W. Liu, D. Liu, and H. Hua, "Key problems of gas-fired power plants participating in peak load regulation: A review," *IET Cyber-Phys. Syst., Theory Appl.*, Dec. 2022, doi: 10.1049/cps2.12042.

[13] S. Wang, X. Li, and Y. Hao, "Coordinated peak regulation control strategy of BESS and thermal power units in high proportion new energy power system," in *Proc. IEEE Sustain. Power Energy Conf. (iSPEC)*, Nov. 2020, pp. 579–584. [Online]. Available: https://ieeexplore.ieee.org/document/9351095

[14] X. Wang and L. Duan, "Peak regulation performance study of the gas turbine combined cycle based combined heating and power system with gas turbine interstage extraction gas method," *Energy Convers. Manag.*, vol. 269, Oct. 2022, Art. no. 116103. [Online]. Available: https://www.sciencedirect.com/science/article/abs/pii/S0196890422008895

[15] B. Prade, "10—Gas turbine operation and combustion performance issues," in *Modern Gas Turbine Systems*. Oxford, U.K.: Woodhead, 2013, pp. 383–423.

[16] A. W. James and S. Rajagopalan, "1—Gas turbines: Operating conditions, components and material requirements," in *Structural Alloys for Power Plants*. Oxford, U.K.: Woodhead, 2014, pp. 3–21.

[17] G. Yin and M. Duan, "Pricing the deep peak regulation service of coal-fired power plants to promote renewable energy integration," *Appl. Energy*, vol. 321, Sep. 2022, Art. no. 119391, doi: 10.1016/j.apenergy.2022.119391.

[18] A. M. Abomazid, N. A. El-Taweel, and H. E. Z. Farag, "Optimal energy management of hydrogen energy facility using integrated battery energy storage and solar photovoltaic systems," *IEEE Trans. Sustain. Energy*, vol. 13, no. 3, pp. 1457–1468, Jul. 2022. [Online]. Available: https://ieeexplore.ieee.org/document/9740444

[19] C. Chen, Y. Li, W. Qiu, C. Liu, Q. Zhang, Z. Li, Z. Lin, and L. Yang, "Cooperative-game-based day-ahead scheduling of local integrated energy systems with shared energy storage," *IEEE Trans. Sustain. Energy*, vol. 13, no. 4, pp. 1994–2011, Oct. 2022. [Online]. Available: https://ieeexplore.ieee.org/document/9783149

[20] A. Mao, T. Yu, Z. Ding, S. Fang, J. Guo, and Q. Sheng, "Optimal scheduling for seaport integrated energy system considering flexible berth allocation," *Appl. Energy*, vol. 308, Feb. 2022, Art. no. 118386. [Online]. Available: https://www.sciencedirect.com/science/article/pii/S030626192101624X

[21] Y. Li, B. Wang, Z. Yang, J. Li, and C. Chen, "Hierarchical stochastic scheduling of multi-community integrated energy systems in uncertain environments via Stackelberg game," *Appl. Energy*, vol. 308, Feb. 2022, Art. no. 118392, doi: 10.1016/j.apenergy.2021.118392.

[22] X. Li, W. Wang, and H. Wang, "Hybrid time-scale energy optimal scheduling strategy for integrated energy system with bilateral interaction with supply and demand," *Appl. Energy*, vol. 285, Mar. 2021, Art. no. 116458, doi: 10.1016/j.apenergy.2021.116458.

[23] C. Liu, C. Wang, Y. Yin, P. Yang, and H. Jiang, "Bi-level dispatch and control strategy based on model predictive control for community integrated energy system considering dynamic response performance," *Appl. Energy*, vol. 310, Mar. 2022, Art. no. 118641, doi: 10.1016/j.apenergy.2022.118641.

[24] Q. Lu, Q. Guo, and W. Zeng, "Optimization scheduling of integrated energy service system in community: A bi-layer optimization model considering multi-energy demand response and user satisfaction," *Energy*, vol. 252, Aug. 2022, Art. no. 124063, doi: 10.1016/j.energy.2022.124063.

[25] V. Sharifi, A. Abdollahi, M. Rashidinejad, E. Heydarian-Forushani, and H. H. Alhelou, "Integrated electricity and natural gas demand response in flexibility-based generation maintenance scheduling," *IEEE Access*, vol. 10, pp. 76021–76030, 2022.

[26] U. Desideri, "3—Fundamentals of gas turbine cycles: Thermodynamics, efficiency and specific power," in *Modern Gas Turbine Systems*. Oxford, U.K.: Woodhead, 2013, pp. 44–85.

[27] L. Lin, X. Tian, and X. Cai, "Gas unit deep peak regulation and power system energy efficiency in consideration of conditional cost," *Autom. Electric Power Syst.*, vol. 42, no. 11, pp. 16–23, Jun. 2018.

[28] B. Zhang, "Low cycle fatigue loss of gas turbine rotor," in *Life Management and Peak-Shaving Operation of Large-Capacity Thermal Power Units*. Beijing, China: Water Conservancy Electric Power Press, 1988, pp. 150–241.

[29] L. Lin and X. Tian, "Analysis of deep peak regulation and its benefit of thermal units in power system with large scale wind power integrated," *Power Syst. Technol.*, vol. 41, no. 7, pp. 2255–2263, 2017.

[30] B. Zhang, "Economy of peak regulating operation of large units," in *Life Management and Peak-Shaving Operation of Large-Capacity Thermal Power Units*. Beijing, China: Water Conservancy Electric Power Press, 1988, pp. 242–275.

[31] C. M. Correa-Posada and P. Sánchez-Martín, "Integrated power and natural gas model for energy adequacy in short-term operation," *IEEE Trans. Power Syst.*, vol. 30, no. 6, pp. 3347–3355, Nov. 2015. [Online]. Available: https://ieeexplore.ieee.org/document/6977991

[32] J. Mi and M. E. Khodayar, "Operation of natural gas and electricity networks with line pack," *J. Modern Power Syst. Clean Energy*, vol. 7, no. 5, pp. 1056–1070, Sep. 2019, doi: 10.1007/s40565-019-0547-0.

[33] Y. Zhang, Y. Hu, J. Ma, and Z. Bie, "A mixed-integer linear programming approach to security-constrained co-optimization expansion planning of natural gas and electricity transmission systems," *IEEE Trans. Power Syst.*, vol. 33, no. 6, pp. 6368–6378, Nov. 2018. [Online]. Available: https://ieeexplore.ieee.org/document/8353140

[34] A. D. Woldeyohannes and M. A. A. Majid, "Simulation model for natural gas transmission pipeline network system," *Simul. Model. Pract. Theory*, vol. 19, no. 1, pp. 196–212, Jan. 2011, doi: 10.1016/j.simpat.2010.06.006.

[35] C. Chen, X. Wu, Y. Li, X. Zhu, Z. Li, J. Ma, W. Qiu, C. Liu, Z. Lin, L. Yang, Q. Wang, and Y. Ding, "Distributionally robust day-ahead scheduling of park-level integrated energy system considering generalized energy storages," *Appl. Energy*, vol. 302, Nov. 2021, Art. no. 117493, doi: 10.1016/j.apenergy.2021.117493.

CHANG LIU received the B.E. degree in electrical engineering from Shandong University, Jinan, China, in 2021. She is currently pursuing the master's degree with the College of Electrical Engineering, Zhejiang University, Hangzhou, China. Her research interests include optimal configuration and scheduling of integrated energy systems, and the restoration strategy of power system based on integrated energy.

YUNCHU WANG received the B.E. degree in electrical engineering from Zhejiang University, Hangzhou, China, in 2020, where she is currently pursuing the Ph.D. degree with the College of Electrical Engineering. Her research interests include demand response mechanism designing and optimization, electricity markets, and power system dispatching and planning under uncertainties.

YUANQIAN MA was born in Chengdu, Sichuan, China, in 1991. She received the B.S. and Ph.D. degrees in electrical engineering and its automation from Sichuan University, Chengdu, in 2014 and 2019, respectively. She was a Visiting Student in electrical power engineering with the University of Alberta for two years. She was a Visiting Scholar with the College of Electrical Engineering, Zhejiang University, in 2021. She is currently a Lecturer with Zhejiang Sci-Tech University, Hangzhou, Zhejiang, China. Her main research interests include demand response and power market.

YUN YANG was born in Guangzhou, Guangdong, China, in 1989. She received the B.S. and M.S. degrees in electrical engineering from Tsinghua University, in 2012 and 2014, respectively. Since 2014, she has been a Senior Engineer with Guangdong Power Grid Company Ltd. She is mainly engaged in power market operation analysis, analysis of power supply and demand situation and risk assessment. She has published 18 articles and granted more than 20 invention patents. She has won the First Prize of the National Energy Chemical Geological System Outstanding Employee Technical Innovation, the Third Prize of the Science and Technology Award of the China Electric Technical Society, and the Second Prize of the Achievement Transformation and Application Award of Southern Power Grid Company.

CHANGMING CHEN received the B.E. degree in electrical engineering from Fuzhou University, Fuzhou, China, in 2019. He is currently pursuing the Ph.D. degree with the College of Electrical Engineering, Zhejiang University, Hangzhou, China. His research interests include power system restoration, configuration and scheduling optimization of integrated energy systems, and shared energy storage technology.

ZHU CHAO was born in Jiujiang, Jiangxi, China, in 1988. He received the B.S. and M.S. degrees in electrical engineering from SCUT, in 2008 and 2011, respectively. Since 2011, he has been a Senior Engineer with Guangdong Power Grid Company Ltd. Since 2021, he has been the Manager of the Operation Planning Department. He is mainly engaged in power market operation analysis, power supply, and demand situation analysis and risk assessment. He has published 14 articles.

LI YANG received the Ph.D. degree in electrical engineering from Zhejiang University, Hangzhou, China, in 2004. She held a postdoctoral position with the Department of Electrical Engineering, Turin Polytechnic University, from 2007 to 2008. She is currently an Associate Professor with the College of Electrical Engineering, Zhejiang University. Her research interests include power market, power system economics, and distribution network planning.

ZHENZHI LIN (Senior Member, IEEE) received the Ph.D. degree in electrical engineering from the South China University of Technology, Guangzhou, China, in 2008. He was a Research Assistant with the Department of Electrical Engineering, The Hong Kong Polytechnic University, from 2007 to 2008, a Research Scholar with the Department of Electrical Engineering and Computer Science, The University of Tennessee, from 2010 to 2011, and a Research Associate with the College of Engineering and Computing Sciences, Durham University, from 2013 to 2014. He is currently a Professor with the College of Electrical Engineering, Zhejiang University, Hangzhou, China. His research interests include power system wide-area monitoring and control, controlled islanding and power system restoration, and data mining in power systems.